

# Global Rewards in Multi-Agent Deep Reinforcement Learning for Autonomous Mobility on Demand Systems

**Heiko Hoppe**

*Technical University of Munich, Germany*

HEIKO.HOPPE@TUM.DE

**Tobias Enders**

*Technical University of Munich, Germany*

TOBIAS.ENDERS@TUM.DE

**Quentin Cappart**

*Polytechnique Montréal, Canada*

QUENTIN.CAPPART@POLYMTL.CA

**Maximilian Schiffer**

*Technical University of Munich, Germany*

SCHIFFER@TUM.DE

## Abstract

We study vehicle dispatching in autonomous mobility on demand (AMoD) systems, where a central operator assigns vehicles to customer requests or rejects these with the aim of maximizing its total profit. Recent approaches use multi-agent deep reinforcement learning (MADRL) to realize scalable yet performant algorithms, but train agents based on local rewards, which distorts the reward signal with respect to the system-wide profit, leading to lower performance. We therefore propose a novel global-rewards-based MADRL algorithm for vehicle dispatching in AMoD systems, which resolves so far existing goal conflicts between the trained agents and the operator by assigning rewards to agents leveraging a counterfactual baseline. Our algorithm shows statistically significant improvements across various settings on real-world data compared to state-of-the-art MADRL algorithms with local rewards. We further provide a structural analysis which shows that the utilization of global rewards can improve implicit vehicle balancing and demand forecasting abilities. Our code is available at <https://github.com/tumBAIS/GR-MADRL-AMoD>.

**Keywords:** multi-agent learning, credit assignment, deep reinforcement learning, autonomous mobility on demand

## 1. Introduction

Within the coming years, in autonomous mobility on demand (AMoD) promises to significantly improve urban passenger transportation. An AMoD system enables its operator to exercise full control over the vehicle fleet, thus improving vehicle dispatching performance, provided that the operator uses an effective control algorithm. This ultimately yields increased vehicle utilization while preserving the comfort of individual mobility. By deciding which requests to accept and assigning vehicles to these requests, the operator faces a contextual multi-stage stochastic control problem. Various approaches to solve this problem exist, ranging from model predictive control (e.g., [Alonso-Mora et al., 2017](#)) to deep reinforcement learning (DRL) (e.g., [Xu et al., 2018](#); [Wang et al., 2018](#); [Enders et al., 2023](#)). The latter shows better performance due to its model-free nature. In this context, multi-agent approaches allow to achieve scalability to large instances. To train the agents' policy, existing work uses local, egoistic, per-agent rewards, which can lead to sub-optimal behavior from the perspective of the central operator interested in maximizing the system-wide profit.

In this work, we improve upon the state-of-the-art local-rewards algorithm (LRA) of [Enders et al. \(2023\)](#) by proposing a novel way to train agents with global rewards. The core of our methodology is a new advantage function, which estimates the individual agents’ contribution to the global reward, as such aligning their goal with the central operator, ultimately following a system-optimal policy. Our algorithm outperforms LRA by up to 2% on average across test dates and up to 6% on individual dates, which is a substantial performance improvement in AMoD. Additionally, our algorithm is as scalable as LRA, accordingly setting a new state-of-the-art for vehicle dispatching in AMoD systems.

### 1.1. Related work

Our work relates to two research streams: from an application perspective to AMoD fleet control, and methodologically to multi-agent deep reinforcement learning (MADRL). We review related literature from both streams in the following.

Algorithms for (A)MoD fleet control range from greedy heuristics (e.g., [Liao, 2003](#); [Lee et al., 2004](#)), to (stochastic) model predictive control (e.g., [Alonso-Mora et al., 2017](#); [Tsao et al., 2018](#)), combinations of optimization and supervised learning (e.g., [Zhang et al., 2017](#); [Jungel et al., 2023](#)), and DRL. Existing DRL-based algorithms differ from our approach, as they often use value-based learning (e.g., [Xu et al., 2018](#); [Wang et al., 2018](#); [Sadeghi Eshkevari et al., 2022](#); [Meneses-Cime et al., 2022](#)), which can decrease learning efficiency and speed. Others focus on explicit rebalancing instead of request assignment (e.g., [Jiao et al., 2021](#); [Liang et al., 2022](#); [He et al., 2022](#)). Furthermore, most previous work considers non-autonomous MoD, aiming to maximize revenues (e.g., [Wang et al., 2018](#); [Xu et al., 2018](#); [Tang et al., 2019](#)), while AMoD should focus on profit maximization (cf. [Enders et al., 2023](#)). Finally, the work of [Enders et al. \(2023\)](#) uses policy-based hybrid MADRL for a profit-maximizing AMoD operator, but trains agents on local rewards, possibly leading to sub-optimal agent behavior. To the best of our knowledge, no work exists that addresses the problem of profit-maximizing vehicle dispatching in AMoD without the aforementioned shortcomings. We address this research gap by extending the work of [Enders et al. \(2023\)](#) to incorporate global rewards, thus creating goal congruence between the agents and the system operator.

A crucial challenge in our setting is deriving per-agent contributions to global success from a shared reward signal, i.e., a credit assignment problem ([Weiß, 1995](#); [Wolpert and Tumer, 1999](#); [Chang et al., 2003](#)). Solution approaches like inverse reinforcement learning (e.g., [Ng and Russell, 2000](#); [Hadfield-Menell et al., 2017](#); [Lin et al., 2018](#)) or value decomposition (e.g., [Kok and Vlassis, 2006](#); [Sunehag et al., 2018](#); [Son et al., 2019](#); [Rashid et al., 2020](#)) are not applicable to our setting, because we cannot observe the behavior of an optimal agent and do not use Q-learning. An alternative approach is reward marginalization, based on difference rewards ([Wolpert and Tumer, 2001](#)), which uses functions (e.g., advantage functions) to estimate the contribution of individual agents to global rewards (e.g., [Nguyen et al., 2018](#); [Wu et al., 2018](#); [Foerster et al., 2018](#)). Reward marginalization approaches often use actor-critic algorithms. However, reward marginalization approaches often suffer from high learning variance and poor sample efficiency, as they are typically built on top of basic DRL algorithms. To the best of our knowledge, no work exists that combines reward marginalization approaches with low-variance actor-critic algorithms so far. We address this research gap by embedding reward marginalization into a Soft Actor-Critic (SAC) framework for discrete actions.

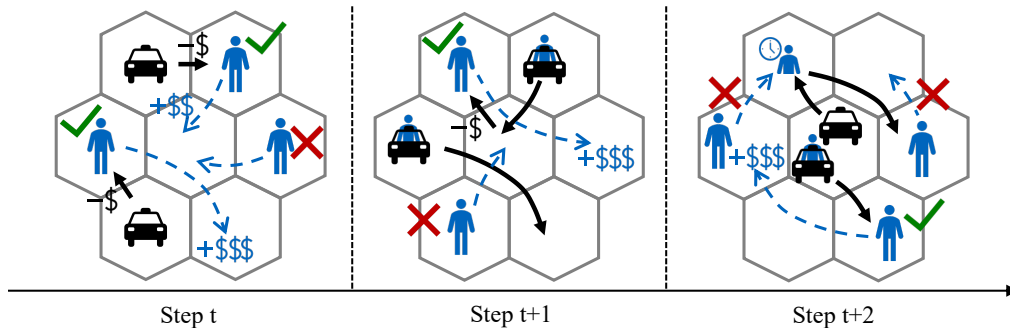


Figure 1: Exemplary vehicle dispatching process.

## 1.2. Contribution

To close the research gap outlined above, we develop the first scalable MADRL-based algorithm for vehicle dispatching in profit-maximizing AMoD that trains agents via global rewards. In this context, we combine SAC for discrete actions with credit assignment based on a counterfactual baseline to resolve goal conflicts between the trained agents and the operator’s global objective. Our algorithm combines the benefits of low learning variance and sample efficiency of SAC with the benefits of credit assignment via a counterfactual baseline. Since this algorithm based on purely global rewards scales only to medium-sized problem instances, we additionally develop a scheduled algorithm that combines local rewards and global rewards with our counterfactual baseline. Thus, we obtain a powerful new MADRL algorithm with possible applications beyond AMoD. We evaluate our algorithm on real-world taxi data from New York City and show that it outperforms LRA of [Enders et al. \(2023\)](#) by up to 2% on average across test dates and up to 6% on individual dates. This constitutes a substantial performance improvement for the AMoD application case, where a single percent improvement yields significant daily monetary gains. We further provide a structural analysis which shows that the utilization of global rewards can improve implicit vehicle balancing and demand forecasting abilities.

## 2. Problem setting

We focus on the contextual multi-stage stochastic control problem from [Enders et al. \(2023\)](#), illustrated in Figure 1, to ensure comparability. In this problem setting, a central operator controls an AMoD fleet and dispatches vehicles to serve requests. We consider a discrete time horizon. During each time step, customers submit a variable number of new requests for point-to-point transportation, of which the operator has no prior knowledge. At the beginning of each time step, the operator makes a decision for the batch of requests that were placed during the previous time step. For each request, this decision is either to reject the request or to assign it to a vehicle. The operator can base its decision on fully observable state information, including the requests’ origins and destinations as well as the vehicles’ positions and already assigned but not yet completed requests. Each request has to be decided upon immediately and customers have a fixed maximum waiting time until they must be picked up. Based on the operator’s decision, the system transitions to the next state: vehicles move towards their next destination and potentially pick up or drop off customers. Customers place new requests, while rejected requests leave the system. We simulate the requests by replaying historical data. Finally, the operator receives the system-wide profit as a reward. The profit is calculated as the sum of all revenues from accepted requests minus the costs for all vehicle movements.

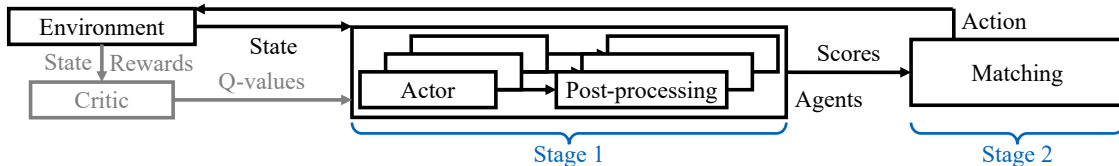


Figure 2: Outline of base algorithm. Black parts are used during training and testing, gray parts only during training.

Revenues and costs are linear functions of the distance travelled. Since fixed costs do not depend on the dispatching problem, we only include operational costs (e.g., for fuel and maintenance). For further details, including a formal Markov decision process, see [Enders et al. \(2023\)](#).

### 3. Methodology

In the following, we first motivate our baseline algorithm (cf. [Enders et al., 2023](#)) and extend it with a naive global reward allocation scheme (Section 3.1). We then focus on reward marginalization and show how to modify the existing Counterfactual Multi-Agent Policy Gradient (COMA) paradigm to SAC architectures (Sections 3.2 & 3.3). We finally discuss enhancements to scale our algorithm to large-scale instances (Section 3.4).

#### 3.1. Base algorithm

Our problem setting has two peculiarities influencing the construction of an effective vehicle dispatching algorithm: the global action space is too large to use single-agent DRL and the number of requests varies between time steps. When addressing the first peculiarity with multi-agent learning, the need for agent coordination arises. The algorithm of [Enders et al. \(2023\)](#) therefore uses a two-stage architecture, see Figure 2. The first stage consists of DRL-trained agents, the second one of an optimization-based central matching. In the first stage, each agent is the combination of a vehicle and a request. An agent can either accept the assignment of the respective request to the respective vehicle or reject this assignment, resulting in a per-agent action space of size two. As the number of requests varies, so does the number of agents. Each agent observes the global state, using an encoding and an attention mechanism to cope with the varying number of requests. Using an actor neural network with a softmax function, the agent obtains probabilities for acceptance and rejection. The per-agent post-processing selects the action by sampling during training or taking the action with the highest probability during testing. It then sets the agent’s score to the acceptance probability in case of an acceptance and to zero in case of a rejection. The scores of all agents are submitted to the global matching, which coordinates the agents. This bipartite matching selects the global action by maximizing the submitted scores under the constraints that every request can be assigned at most once and that every vehicle can take at most one new request.

We train the agents using SAC for discrete actions ([Haarnoja et al., 2018](#); [Christodoulou, 2019](#)). As the use of multiple agents only serves to handle the large action space, we train a single actor and a single critic network and use them for all agents. The rewards we use for training are the profits obtained by the algorithm: when a request is assigned to a vehicle and served within the maximum waiting time, the respective agent immediately receives the profit as a reward.

To transition from this algorithm to our contribution, we first follow a naive approach to include global rewards in training by replacing the per-agent rewards with global rewards when training the critic, resulting in a basic global rewards algorithm (GRA). We obtain global rewards by summing

the profits of all agents at one time step. As this number can be substantially larger than per-agent rewards, we divide it by the average number of non-zero rewards per observation in the replay buffer to stabilize learning. Straightforwardly using this approach leads to a credit assignment problem, as the reward given to agents now depends on the actions of all agents, which generally complicates an agent’s learning task. To mitigate this, we explore a credit assignment paradigm in the following.

### 3.2. Naive COMA

A suitable credit assignment paradigm for our setting is COMA, proposed by Foerster et al. (2018). COMA fits our setting best, because it has a similar structure as SAC and is especially suitable for small per-agent action spaces. Following the main rationale of COMA, agents should maximize their contribution to the global reward instead of maximizing the global reward directly. As obtaining global rewards for several actions is computationally infeasible, COMA trains the critic on global rewards to approximate global state-action-values. The contribution of an agent to this global value is defined as the value of taking an action in contrast to the value of taking a default action. This default action is calculated as the policy-weighted average value of all possible actions the agent can take (counterfactual baseline). The advantage function of COMA therefore is

$$A_i(a_i|s, i) = Q_\theta(a_i|s, \bar{a}_{-i}) - \sum_{a'_i} \pi_\phi(a'_i|s, i) Q_\theta(a'_i|s, \bar{a}_{-i}). \quad (1)$$

In this and all following equations,  $s$  denotes the global state,  $a'_i$  an action agent  $i$  can take as a reject/accept decision before the global matching,  $a_i$  the action the agent actually takes, and  $\bar{a}_{-i}$  the actions of all agents except agent  $i$  after the global matching. Let  $\pi_\phi(a_i|s, i) \in [0, 1]$  be the probability that agent  $i$  takes action  $a_i$  in state  $s$ , following policy  $\pi_\phi$  parameterized by network  $\phi$ .  $Q_\theta(a_i|s, \bar{a}_{-i}) \in \mathbb{R}^2$  is the global state-action-value (Q-value) of action  $a_i$  taken by agent  $i$  in state  $s$  estimated using network  $\theta$ , given other agents’ actions  $\bar{a}_{-i}$ .

Foerster et al. (2018) use a sampling-based approach to estimate the actor’s loss function and base its computation only on the action taken by the agent. The loss function thus reads  $J_\pi(\phi) = \mathbb{E}_{s \sim D} [\sum_i A_i(a_i|s, i)]$ , with  $D$  denoting the replay buffer. In contrast to that, Enders et al. (2023) use SAC with discrete actions, which considers all possible actions of an agent in the loss function

$$J_\pi(\phi) = \mathbb{E}_{s \sim D} \left[ \sum_i \sum_{a_i} \pi_\phi(a_i|s, i) \left( \alpha \log \pi_\phi(a_i|s, i) - \min_{j \in \{1, 2\}} \left\{ Q_\theta^j(a_i|s, \bar{a}_{-i}) \right\} \right) \right], \quad (2)$$

with  $\alpha \in \mathbb{R}$  being the entropy coefficient. To use credit assignment via COMA in combination with the proven reliability and low variance of SAC, we need to integrate the baseline of COMA into the loss function of SAC. In the following, we use  $\pi(a_i) := \pi_\phi(a_i|s, i)$  and  $Q(a_i) := \min_{j \in \{1, 2\}} \left\{ Q_\theta^j(a_i|s, \bar{a}_{-i}) \right\}$  for conciseness. Then, considering one instance of a batch and one agent, the loss function of SAC extended by the advantage of COMA reads

$$J_\pi(\phi|s, i) = \sum_{a_i} \pi(a_i) \left( \alpha \log \pi(a_i) - Q(a_i) + \sum_{a'_i} \pi(a'_i) Q(a'_i) \right). \quad (3)$$

**Proposition 1** *The loss function  $J_\pi(\phi|s, i)$  as defined in Equation (3) is equivalent to the entropy  $J_\pi(\phi|s, i) = \sum_{a_i} \pi(a_i) \alpha \log \pi(a_i)$  of a plain SAC architecture.*

For a proof of Proposition 1, we refer to Appendix A. Accordingly, using the loss function as derived in Equation (3) does not allow to learn a meaningful policy such that we cannot straightforwardly apply the COMA paradigm to our SAC framework. This observation motivates us to study a novel approach to combine SAC for discrete actions with the COMA paradigm to learn a good policy with global rewards.

### 3.3. Adjusted COMA for SAC architectures

To solve the convergence problem outlined above, we have to adjust the loss function in Equation (3). Using only the action taken by the agent for the loss function as in Foerster et al. (2018) does not lead to convergence even in small experimental instances, as it increases the loss function’s variance. We therefore adjust  $\pi(a'_i)$ , changing the weighting of the default action in the baseline. This is possible from a theoretical perspective, as the exact specification of a default action is not derived from the idea of difference rewards (Wolpert and Tumer, 2001), but left to the discretion of the user.

Straightforwardly, we can define the default action by using an equally-weighted average instead of a policy-weighted average, resulting in the advantage function  $A_i^{\text{equ}}(a_i) = Q(a_i) - \sum_{a'_i} \frac{1}{n_{a_i}} Q(a'_i)$ , with  $n_{a_i}$  being the number of actions per agent. We call this algorithm  $\text{COMA}^{\text{equ}}$ , which resolves the convergence problem, but has a disadvantage: when the actor network estimates different probabilities for single actions, weighting all actions equally is not a reasonable default action. This problem is especially pronounced during late training, when the actor network is better at estimating action probabilities. We solve this issue by defining a second default action with the use of a target actor network  $\bar{\phi}$ . This network has the same structure and initialization as the actor network  $\phi$  and is updated using exponential averages of the actor network’s parameters, similar to target networks in Q-learning. The advantage function of this algorithm ( $\text{COMA}^{\text{tgt}}$ ) is  $A_i^{\text{tgt}}(a_i) = Q(a_i) - \sum_{a'_i} \pi_{\bar{\phi}}(a'_i) Q(a'_i)$ . Since  $\bar{\phi}$  differs from  $\phi$ , this algorithm solves the convergence problem as well. During early training,  $\text{COMA}^{\text{tgt}}$  is not as suitable as  $\text{COMA}^{\text{equ}}$ , since the sub-optimal action probabilities of an untrained target actor network are a disadvantage compared to equally-weighted actions. Later in training,  $\bar{\phi}$  can estimate better action probabilities, making  $\text{COMA}^{\text{tgt}}$  superior to  $\text{COMA}^{\text{equ}}$ .

Since we now have one algorithm especially suitable for early learning and one especially suitable for later learning, we combine these two and obtain  $\text{COMA}^{\text{adj}}$ , based on a dynamic combination of the two newly introduced advantage functions. The advantage function of  $\text{COMA}^{\text{adj}}$  thus reads

$$\begin{aligned} A_i^{\text{adj}}(a_i) &= (1 - \beta)A_i^{\text{equ}}(a_i) + \beta A_i^{\text{tgt}}(a_i) \\ &= Q(a_i) - (1 - \beta) \sum_{a'_i} \frac{1}{n_{a_i}} Q(a'_i) - \beta \sum_{a'_i} \pi_{\bar{\phi}}(a'_i) Q(a'_i). \end{aligned} \tag{4}$$

Here, the hyperparameter  $\beta \in [0, 1]$  is the weight of the  $\text{COMA}^{\text{tgt}}$  baseline and follows a schedule, starting at zero and ending at one, see Appendix B.3. Then, the loss function of  $\text{COMA}^{\text{adj}}$  reads

$$J_{\pi}^{\text{adj}}(\phi|s, i) = \sum_{a_i} \pi(a_i) \left( \alpha \log \pi(a_i) - A_i^{\text{adj}}(a_i) \right). \tag{5}$$

With this loss function,  $\text{COMA}^{\text{adj}}$  solves the credit assignment problem. In our experiments,  $\text{COMA}^{\text{adj}}$  performs better than LRA, but has a scalability problem: when the number of agents

increases beyond medium-sized problem instances, COMA<sup>adj</sup> fails to converge. Reasons for this are the diminishing influence of a single agent on global rewards and the overlap of many agents’ actions when the number of agents increases, making learning per-agent Q-values difficult (cf. [Rashid et al., 2020](#)). We therefore investigate how to scale COMA<sup>adj</sup>.

### 3.4. Reward scheduling

Usually, one could resolve the scalability problem of COMA<sup>adj</sup> straightforwardly by adjusting the critic to accommodate value factorization (e.g., [Su et al., 2021](#)), but this approach is infeasible in our setting as the number of agents is variable. Similarly, learning the critic on a static mix of local and global rewards in a local-global-rewards algorithm (LGRA) does not solve the scalability problem, since any non-negligible share of global rewards distorts learning when increasing the number of agents. In addition, reward marginalization with a counterfactual baseline is problematic for partially local rewards.

Instead, we can train a single actor network using a weighted average policy loss function, consisting of the loss function for LRA,  $J_{\pi}^{\text{loc}}(\phi|s, i)$ , by [Enders et al. \(2023\)](#) and COMA<sup>adj</sup>. The loss function thus reads

$$J_{\pi}^{\text{scd}}(\phi|s, i) = (1 - \kappa) J_{\pi}^{\text{loc}}(\phi|s, i) + \kappa J_{\pi}^{\text{adj}}(\phi|s, i), \quad (6)$$

with  $\kappa \in [0, 1]$  being the weight of the loss function of COMA<sup>adj</sup>. Again,  $\kappa$  follows a schedule increasing linearly, following a polynomial pattern or jumping from zero to one at a specified point, see [Appendix B.3](#). This leads to a new algorithm, we call it COMA<sup>scd</sup>. COMA<sup>scd</sup> solves the scalability problem, as it enables the learning of global Q-values when increasing the number of agents. The reason this works is the utilization of experience collected following a mixed policy: this way, more diverse experience is available than if using solely own experience, thus improving learning without the destabilizing influence of increasing the entropy. We can therefore train four critic networks from the beginning on, two for local and two for global rewards. Two networks each are necessary for SAC, where we always use the minimum of the two state-action-values to avoid value overestimation. Due to the influence of both local and global rewards, COMA<sup>scd</sup> can sometimes have a lower performance than algorithms purely based on global rewards, but makes up for this by being as scalable as LRA, thus sacrificing a portion of its performance for scalability.

## 4. Numerical studies

We benchmark our algorithms using the experimental design of [Enders et al. \(2023\)](#), which bases on New York Taxi data ([NYC TLC, 2015](#)) in a hexagonal grid of Manhattan, with 38 large, 11 small, or 5 small zones. In this realm, we study five instances: two edge cases with high (5 zones, 15 vehicles) and low (11 zones, 6 vehicles) acceptance rates, two typical test cases (11 zones, 18 and 24 vehicles), and a comparatively large instance (38 zones, 100 vehicles). For details on the experimental design, we refer to [Appendix B.1](#) and report hyperparameters for all models in [Appendix B.2](#).

Firstly, we test COMA<sup>scd</sup> on all five instances and benchmark it against LRA of [Enders et al. \(2023\)](#) and a greedy algorithm, which considers requests in their order of submission, accepting profitable ones and rejecting all others. Secondly, we present an ablation study to show the superiority of COMA<sup>scd</sup> over our alternative algorithms that use global rewards. Thirdly, we discuss why COMA<sup>scd</sup> outperforms LRA.

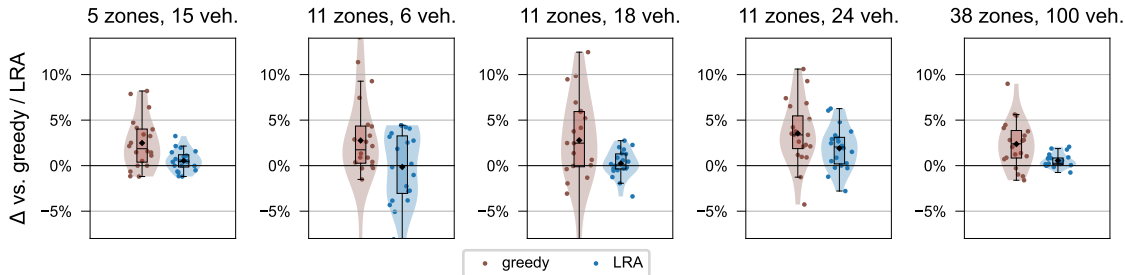


Figure 3: Relative test performance  $\Delta$  [%] of  $\text{COMA}^{\text{scd}}$  vs. greedy and LRA for multiple test dates.

	5 zones, 15 veh.	11 zones, 6 veh.	11 zones, 18 veh.	11 zones, 24 veh.	38 zones, 100 veh.
vs. LRA	0.5%	-0.2%	0.2%	1.9%	0.6%
p-value	0.05	0.52	0.22	0.00	0.00
vs. greedy	2.5%	2.8%	2.8%	3.5%	2.4%
p-value	0.00	0.00	0.01	0.00	0.00

Table 1: Mean test performance improvement of  $\text{COMA}^{\text{scd}}$  vs. LRA and greedy, including the respective Wilcoxon p-values.

#### 4.1. Performance of $\text{COMA}^{\text{scd}}$

We present results of our tests of  $\text{COMA}^{\text{scd}}$  in Figure 3 and Table 1. In all instances except the one with 11 zones and 6 vehicles,  $\text{COMA}^{\text{scd}}$  outperforms LRA and the greedy algorithm on average, the former by up to 1.9% and the latter by up to 3.5%. On single test dates,  $\text{COMA}^{\text{scd}}$  can outperform LRA by up to 6%. This improvement is significant, as the Wilcoxon p-values are at most 5% for the respective instances. While these relative improvements appear to be small, they are substantial in AMoD and of a similar magnitude as the improvements of previous state-of-the-art algorithms over their respective benchmarks (cf. [Sadeghi Eshkevari et al., 2022](#); [Enders et al., 2023](#)).

In the instance with a high acceptance rate (5 zones, 15 vehicles), the significant performance improvement of  $\text{COMA}^{\text{scd}}$  compared to LRA is an especially positive result, as a vehicle is usually available for each request in this instance, limiting the improvement potential for DRL. In the instance with a low acceptance rate (11 zones, 6 vehicles), the improvement potential is similarly limited, as vehicles are rarely idle. Consequently, the performance of  $\text{COMA}^{\text{scd}}$  is most similar to LRA in this instance. In contrast, the instance of 11 zones and 24 vehicles has a balanced ratio between the number of vehicles and requests. Here, the performance improvement of  $\text{COMA}^{\text{scd}}$  is the largest of all instances, outperforming LRA by on average 1.9% and greedy by on average 3.5%. In the large instance (38 zones, 100 vehicles),  $\text{COMA}^{\text{scd}}$  significantly improves performance by on average 0.6% compared to LRA, proving that the algorithm is applicable to large-scale environments. The lower performance improvement can be explained by the weight of  $\text{COMA}^{\text{adj}}$  being required to increase more slowly in the loss function of  $\text{COMA}^{\text{scd}}$  when the number of agents increases.

#### 4.2. Ablation study

In the following, we discuss the performance of all proposed algorithms with respect to numerical stability and scalability across random seeds (Table 2) as well as computational performance (Table 3 & Figure 4). As can be seen in Table 2, all algorithms show stable convergence for the small instances, while all but LRA, LGRA, and  $\text{COMA}^{\text{scd}}$  exhibit stability issues already for medium-sized instances, failing to converge for one-third of the seeds and requiring about ten times as many training steps to converge compared to LRA for the remaining seeds. In contrast, LGRA



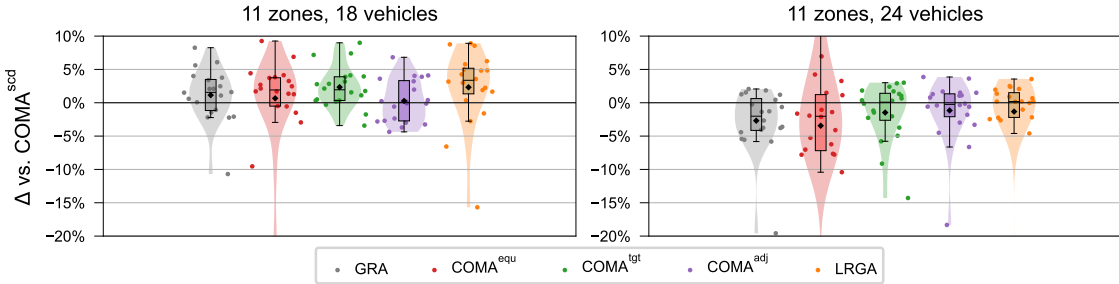


Figure 4: Relative test performance  $\Delta$  [%] of all algorithms vs.  $COMA^{scd}$ .

	5 zones 15 veh.	11 zones 6 veh.	11 zones 18 veh.	11 zones 24 veh.	38 zones 100 veh.	11 zones	
						18 vehicles	24 vehicles
GRA	✓	✓	○	○	–	1.2% (0.02)	-2.7% (0.01)
$COMA^{equ}$	✓	✓	○	○	–	0.7% (0.03)	-3.5% (0.04)
$COMA^{tgt}$	✓	✓	○	○	–	2.3% (0.00)	-1.5% (0.23)
$COMA^{adj}$	✓	✓	○	○	–	0.3% (0.42)	-1.2% (0.41)
LRGA	✓	✓	✓	✓	–	2.3% (0.00)	-1.3% (0.55)
LRA	✓	✓	✓	✓	✓		
$COMA^{scd}$	✓	✓	✓	✓	✓		

Table 2: Convergence of algorithms. ✓ denotes stable convergence, ○ unstable convergence (across random seeds), – no convergence.

Table 3: Test performance of algorithms vs.  $COMA^{scd}$  (Wilcoxon p-value).

and  $COMA^{scd}$  converge on all seeds and require comparable to at maximum twice as many training steps compared to LRA. For the large instance, only  $COMA^{scd}$  and the LRA baseline converge, with  $COMA^{scd}$  again requiring similar to twice as many training steps. Figure 4 and Table 3 show the relative performance of all algorithms compared to  $COMA^{scd}$  for the medium-sized instances over seeds for which all algorithms converged. As can be seen, the results are mixed: while pure global-rewards-based algorithms outperform  $COMA^{scd}$  on average on the 18 vehicles instance,  $COMA^{scd}$  outperforms all other algorithms on the 24 vehicles instance. To understand this ambiguous effect, we need to detail the algorithms’ convergence behavior: increasing the instance from 18 to 24 vehicles technically requires to train 570 instead of 430 agents, which significantly challenges all purely global-rewards-based algorithms. In fact, if one looks at the variance of the validation reward of each algorithm (see Appendix B.4), we observe converging but less stable learning behavior for all purely global-rewards-based algorithms, which explains the respective performance drop. While this observation manifests the robustness of  $COMA^{scd}$  at a performance that improves upon local-rewards-based algorithms, it also points at a promising direction for future research: if one manages to stabilize and scale the purely global-rewards-based algorithms, one will most likely obtain even better performing algorithms.

### 4.3. Structural analysis

Finally, we aim to understand the performance difference between the studied algorithms by analyzing the respective policy characteristics in Table 4, which details request rejection rates for our LRA baseline, the pure global-rewards-based algorithm  $COMA^{adj}$ , and  $COMA^{scd}$ . As can be seen, both  $COMA$ -based algorithms have a lower rejection rate compared to LRA, which explains their improved performance. This finding, as well as the relation between  $COMA^{scd}$  and  $COMA^{adj}$ , are in line with the performance shown for the 24 vehicles instance in Figure 4. To understand operational

measure	LRA	COMA <sup>adj</sup>	COMA <sup>scd</sup>
rejection rate	17.6%	16.6%	15.5%
→ rejection rate for destination zones without vehicles	16.4%	12.9%	13.6%
→ rejection rate for destination zones with >2 vehicles	20.2%	19.3%	18.5%
ratio of overperformance rejections / acceptances	1.75	1.87	1.27

Table 4: Rejection rates of generally profitable requests on the instance with 24 vehicles.

intricacies, we further analyze the difference between average rejection rates of empty destination zones and zones that contain more than two vehicles upon a request’s arrival, which is 3.8% for LRA, 6.4% for COMA<sup>adj</sup> and 4.9% for COMA<sup>scd</sup>. This indicates a stronger focus of COMA<sup>scd</sup> and COMA<sup>adj</sup> on implicit vehicle balancing, as these algorithms are more reluctant to send vehicles to already crowded zones. Such a focus on vehicle balancing stems from global reward structures and partially explains performance improvements: if vehicles are unbalanced, less overall requests can be served; individual vehicles might still obtain high local rewards, but the global reward decreases.

Beyond implicit balancing, we analyze the algorithms’ anticipative performance, i.e., their capability to foresee future demand and consider it during decision-making. To do so, we analyze an algorithm’s overperformance ratio (see Table 4), which compares the summed theoretical profits of future requests in the same zone following acceptance or rejection of an initially profitable request. We calculate this ratio by dividing the total theoretical profit after rejections by that after acceptances (see Appendix B.5 for details). As can be seen, COMA<sup>adj</sup> has the highest overperformance ratio, followed by LRA and COMA<sup>scd</sup>. From the higher ratio, we conclude that COMA<sup>adj</sup> has better forecasting abilities, as requests after rejections are more profitable than requests after acceptances under its policy. In contrast, COMA<sup>scd</sup> appears to suffer from the mixture of local and global rewards, which can explain some of the performance gaps compared to algorithms with purely global rewards. A possible reason for the better forecasting abilities of COMA<sup>adj</sup> is that global Q-values incorporate more prescriptive information: since global rewards are less dependent on the actions of individual agents, it is easier to infer information about demand from them, such that agents trained using global Q-values might have access to better demand predictions.

## 5. Conclusion

We study vehicle dispatching for AMoD systems, where a profit-maximizing central operator assigns vehicles to requests or rejects these. We propose a novel MADRL algorithm with global rewards and credit assignment based on a counterfactual baseline. Our algorithm combines the benefits of low learning variance and sample efficiency of SAC with the benefits of credit assignment of COMA. We show that a naive combination of SAC and COMA does not converge, and develop a stable and scalable algorithm that uses reward scheduling with a new advantage function based on an equally-weighted baseline and a target actor network baseline. We show that our algorithm improves upon the current state-of-the-art by up to 2% on average across test dates and up to 6% on individual dates from real-world data sets. This constitutes a substantial performance improvement for the AMoD application case where a single percent improvement yields significant daily monetary gains. We further provide a structural analysis which shows that the use of global rewards can improve implicit vehicle balancing and demand forecasting abilities. Our proposed algorithm is applicable beyond the area of AMoD, as it can be useful in any application where stable multi-agent deep reinforcement learning with credit assignment is required. Future work may apply our algorithm to other areas or focus on stabilizing purely global-rewards-based algorithms.

## Appendix A. Proof of Proposition 1

The combined loss function of SAC and COMA for one instance of a batch and one agent is

$$J_{\pi}(\phi|s, i) = \sum_{a_i} \pi(a_i) \left( \alpha \log \pi(a_i) - Q(a_i) + \sum_{a'_i} \pi(a'_i) Q(a'_i) \right).$$

Considering the last summand separately, we get

$$\begin{aligned} & \sum_{a_i} \pi(a_i) \sum_{a'_i} \pi(a'_i) Q(a'_i) \\ &= \pi_1 (\pi_1 Q_1 + \pi_2 Q_2 + \dots + \pi_n Q_n) + \dots + \pi_n (\pi_1 Q_1 + \pi_2 Q_2 + \dots + \pi_n Q_n) \\ &= \pi_1^2 Q_1 + \pi_1 \pi_2 Q_2 + \dots + \pi_1 \pi_n Q_n + \pi_2 \pi_1 Q_1 + \dots + \pi_n \pi_1 Q_1 + \dots + \pi_n^2 Q_n \\ &= \pi_1 Q_1 (\pi_1 + \pi_2 + \dots + \pi_n) + \dots + \pi_n Q_n (\pi_1 + \pi_2 + \dots + \pi_n) \\ &= \sum_{a_i} \pi(a_i) Q(a_i). \end{aligned}$$

Inserting that into the loss function, we obtain

$$J_{\pi}(\phi|s, i) = \sum_{a_i} \pi(a_i) \alpha \log \pi(a_i) - \sum_{a_i} \pi(a_i) Q(a_i) + \sum_{a_i} \pi(a_i) Q(a_i) = \sum_{a_i} \pi(a_i) \alpha \log \pi(a_i),$$

which is just the entropy. If the loss function equals the entropy, the actor is not trained to maximize the probabilities of actions associated with the highest Q-values and thus cannot learn a meaningful policy. Note that this problem occurs for an arbitrary number of  $n$  actions per agent (as displayed), including our setting with  $n = 2$  actions.

## Appendix B. Experiments

### B.1. Experimental setup

**Data:** We use the same experimental setup as [Enders et al. \(2023\)](#): our data consists of yellow taxi trip records from 2015, excluding weekends and holidays. We define the time of request placement as the pickup time in the data set, and consider a one hour time interval per day as one episode, using a time step size of one minute. We discretize the island of Manhattan using small or large hexagonal zones. Neighboring zones' centers have a distance of 459 or 917 meters for the small and large zones, respectively. In our instances, 38 large zones roughly cover the southern two thirds of Manhattan, 11 small zones cover roughly three square kilometers in central Manhattan and 5 small zones denote the southern five of these zones, covering close to half of that area. For each instance, we delete all requests originating in or leading to zones outside the area under consideration and all requests that start and end within the same zone. Vehicles travel along the shortest route between zones. We assume a travel time of two time steps between neighboring small zones and five time steps between neighboring large zones. The maximum waiting time of customers between request submission and pickup is five minutes. We set the revenue to 5.00 USD per km and the costs to 4.50 USD per km, resulting in a profit margin of 10% in ideal cases. The maximum number of requests per time step never exceeds 7 for the instances with 5 small zones and 24 for the instances of 11 small zones. For the instances of 38 large zones, we use only every 20<sup>th</sup> request to make the problem size tractable for our available hardware. This results in a maximum of 20 requests per time step in these instances.

**Hardware:** We train the models on NVIDIA Tesla P100, V100, or A100 GPUs. Depending on the problem size and number of time steps for training, this training takes between 2 and 66 hours.

**Benchmark:** The greedy algorithm considers all requests in the order of their arrival. If a vehicle is available to serve the request with a positive profit and within the maximum waiting time, it is assigned to serve the request. If there are multiple available vehicles, the greedy algorithm assigns the vehicle that can serve the request with the highest profit. If no vehicle is available, the greedy algorithm rejects the request. In the instance with 5 zones and 15 vehicles, the greedy algorithm accepts 78% of requests. This acceptance rate is 22% in the instance with 11 zones and 6 vehicles, 47% in the instance with 11 zones and 18 vehicles, 55% in the instance with 11 zones and 24 vehicles, and 50% in the instance with 38 zones and 100 vehicles.

## B.2. Hyperparameters

We mostly use the same hyperparameters as [Enders et al. \(2023\)](#) for our algorithm, only adjusting the entropy coefficient  $\alpha$ , the learning rate, and the total number of training steps. A different number of random steps in the beginning, size of the replay buffer, batch size, or discount factor did not improve our results.

We train models until their validation performance is stable and does not increase further. Depending on the instance and algorithm, this results in 200,000 to 2,000,000 training steps. The number of required steps increases with the instance size, i.e., with the number of zones and vehicles. Across instances, LRA, COMA<sup>scd</sup> and LGRA require 200,000 to 400,000 steps, while GRA, COMA<sup>equ</sup>, COMA<sup>tgt</sup> and COMA<sup>adj</sup> require 200,000 to 2,000,000 steps. We separate the learning rates for actor and critic, as global rewards and the inclusion of a baseline can change the models’ convergence properties. Tuning the learning rates for each instance, we set both learning rates to  $3 \cdot 10^{-4}$  for LRA and to values between  $3 \cdot 10^{-4}$  and  $2.4 \cdot 10^{-3}$  for GRA. For the algorithms based on COMA (COMA<sup>equ</sup>, COMA<sup>tgt</sup>, COMA<sup>adj</sup>, COMA<sup>scd</sup>), we set the learning rates to values between  $6 \cdot 10^{-4}$  and  $1.8 \cdot 10^{-3}$ , with the actor having higher learning rates than the critic. We further tune the entropy coefficient  $\alpha$  for each instance, with values ranging between 0.37 and 1.5.

At the end of each training run, we test the model with the best validation performance on the test data. The score of a single test date is the sum of all individual scores on that date. We repeat each training run with three different random seeds and average test scores over these random seeds. If a run does not converge to a reasonable performance, we exclude it from the average. This only applies to some of the algorithms in the ablation study in Section 4.2. All test scores in this paper are obtained in that way.

## B.3. Training schedules

The policy loss function of COMA<sup>adj</sup> is a dynamic weighted average of the loss functions of COMA<sup>equ</sup> and COMA<sup>tgt</sup>, with  $\beta$  being the weight of the loss function of COMA<sup>tgt</sup>. Over the course of the training,  $\beta$  always starts at zero, ends at one, and can increase linearly or following a power function. Since COMA<sup>tgt</sup> shows better experimental performance than COMA<sup>equ</sup> (see Section 4.2), we test a power function with an exponent of 0.5 to increase the share of COMA<sup>tgt</sup> quicker than when using a linear schedule. In the instance of 11 zones and 18 vehicles, the maximum average performance of a model with a power function is 4.6% lower than the maximum average performance of a model with a linear function. In the instance of 11 zones and 24 vehicles, this number is 2.8%. We conclude that a linearly increasing  $\beta$  works best.

The policy loss function of  $\text{COMA}^{\text{scd}}$  is a dynamic weighted average of the loss functions of LRA and  $\text{COMA}^{\text{adj}}$ , with  $\kappa$  being the weight of the loss function of  $\text{COMA}^{\text{adj}}$ . Over the course of the training,  $\kappa$  always starts at zero and ends at one. It can increase linearly, following a power function, or it can jump from zero to one at any specified point during training. We present results of tests for different patterns of increasing  $\kappa$  in Table 5. We draw four conclusions from these tests: firstly, power functions generally lead to the best performance, which is most likely the result of their smoother transition from local to global rewards in comparison to sudden jumps. Secondly, quickly increasing power functions with exponents between 0.01 and 0.5 work best in all instances. As a result of these quickly increasing functions, the share of  $\text{COMA}^{\text{adj}}$  in the loss function rises faster in the best models than it would when following a linear schedule. This shows that a quick transition to global rewards enables utilizing their benefits for a larger part of the training. Thirdly, the best exponents vary between instances, i.e., a per-instance tuning of the schedule to increase  $\kappa$  can lead to visible performance increases. Finally, the best performing exponent increases with the instance size. We thus conclude that large instances require a slower transition from local to global rewards to achieve best performance, in line with our results concerning the scalability problems of global-rewards-based algorithms.

#### B.4. Validation rewards

We show the validation rewards of GRA,  $\text{COMA}^{\text{equ}}$ ,  $\text{COMA}^{\text{tgt}}$ ,  $\text{COMA}^{\text{adj}}$ , LGRA, LRA, and  $\text{COMA}^{\text{scd}}$  for the instance with 11 zones and 18 vehicles and the instance with 11 zones and 24 vehicles over the course of training in Figure 5. We observe three patterns in the validation rewards: firstly, in both instances, the purely global-rewards-based algorithms GRA,  $\text{COMA}^{\text{equ}}$ ,  $\text{COMA}^{\text{tgt}}$ , and  $\text{COMA}^{\text{adj}}$  need about ten times as many training steps to converge as LRA, while LGRA and  $\text{COMA}^{\text{scd}}$  need about the same to double the number of steps until convergence. Secondly, most purely global-rewards-based algorithms display far larger differences between their best and worst validation performance in both instances, indicating unstable convergence behavior. Finally, the convergence speed decreases for the purely global-rewards-based algorithms except  $\text{COMA}^{\text{adj}}$  in the instance with 24 vehicles compared to the one with 18 vehicles. For  $\text{COMA}^{\text{adj}}$ , the maximum and minimum performance diverges more in the larger instance. The algorithm LGRA also faces challenges when increasing the number of agents: to remain stable and converge quickly, we have to decrease the share of global rewards from 60% to 30%, thereby also lowering the positive influence of global rewards. In contrast, LRA and  $\text{COMA}^{\text{scd}}$  have about the same stability and convergence speed in both instances.

This final observation provides evidence for the lower performance of purely global-rewards-based algorithms in the instance with 24 vehicles. As the learning is less stable, the learned policies are less reliable. With even validation performance curves of converging models being less stable, trained models are more likely to converge to a sub-optimal policy. While we allow all algorithms enough steps to converge, the slower learning of purely global-rewards-based algorithms can be an additional problem in practice. Overall, these results confirm our conclusion that learning using purely global rewards increases vehicle dispatching performance, but leads to problems when increasing the number of agents.

instance	schedule type	exponent/jump	vs. best
5 zones, 15 veh.	<b>power</b>	<b>0.01</b>	<b>0.0%</b>
	power	0.05	-1.5%
	power	0.25	-1.6%
	jump	0.01	-1.9%
11 zones, 6 veh.	<b>power</b>	<b>0.25</b>	<b>0.0%</b>
	jump	0.01	-0.7%
	power	0.125	-1.6%
	jump	0.02	-2.1%
11 zones, 18 veh.	power	0.01	-4.4%
	<b>power</b>	<b>0.25</b>	<b>0.0%</b>
	jump	0.1	-0.4%
	jump	0.25	-0.4%
	power	2.00	-0.6%
11 zones, 24 veh.	power	1.00	-1.2%
	power	0.50	-2.1%
	jump	0.50	-3.1%
	<b>power</b>	<b>0.25</b>	<b>0.0%</b>
11 zones, 24 veh.	jump	0.125	-1.0%
	power	0.125	-1.6%
	power	1.00	-1.7%
	<b>power</b>	<b>0.5</b>	<b>0.0%</b>
38 zones, 100 veh.	power	1.00	-0.2%
	power	0.25	-0.3%
	jump	0.25	-0.3%
	power	0.25	-0.3%

Table 5: Performance of training schemes of COMA<sup>scd</sup>, relative to the best performance per instance. The specifications used in Sections 4.1 to 4.3 are displayed in bold writing. The column exponent/jump denotes the exponent in case of a power function or the jump point relative to the number of training steps in case of a jump schedule. For example, if the jump point is 0.25 and the model is trained for 400,000 steps,  $\kappa$  is zero for the first 100,000 steps and one for the remainder of the training.

GLOBAL REWARDS IN MADRL FOR AMoD

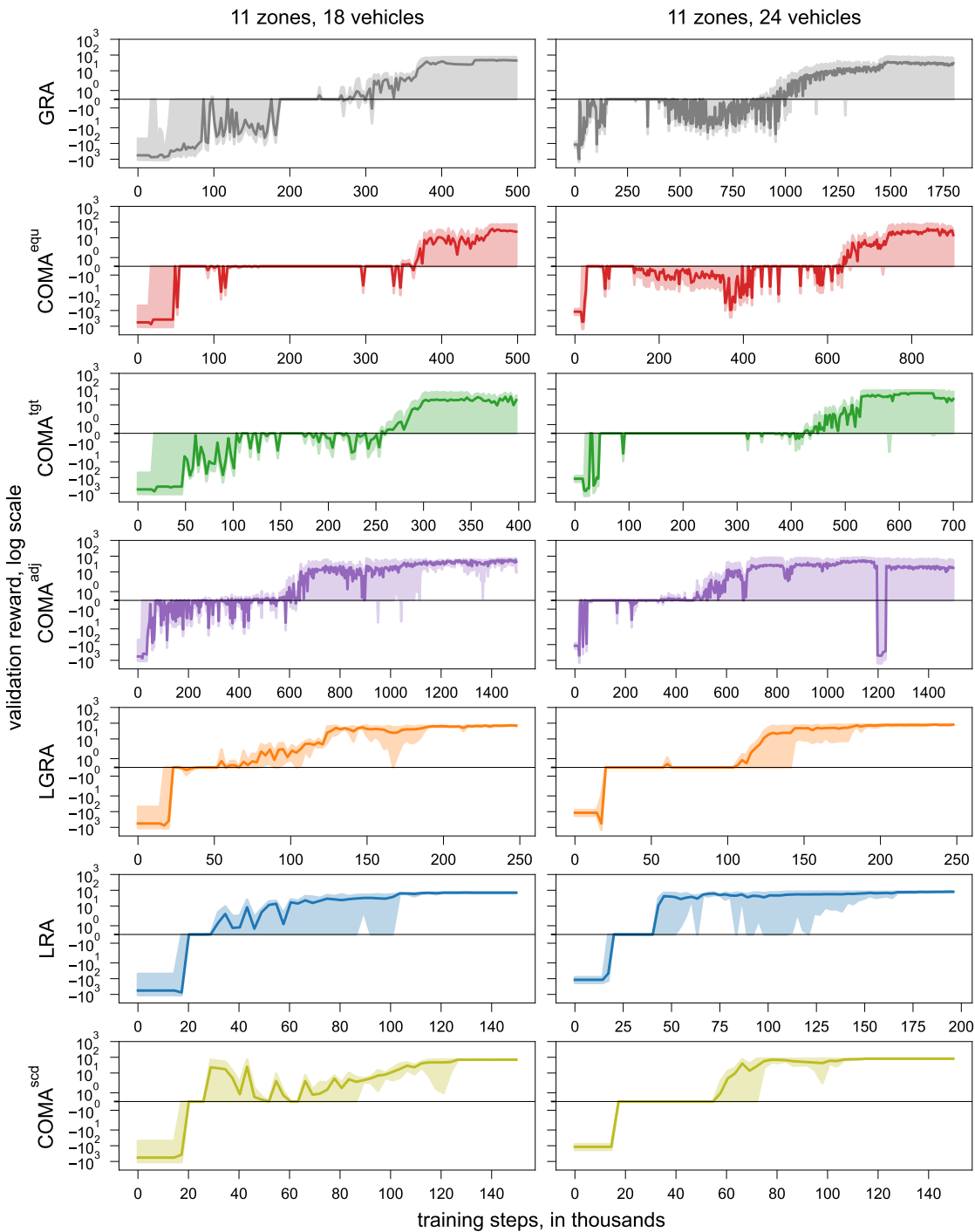


Figure 5: Validation rewards of algorithms over training steps. The black horizontal line indicates zero. The main line denotes the average validation reward over the three random seeds, the shaded area the maximum and minimum rewards at each step.

### B.5. Calculation of overperformance ratio

We calculate the overperformance ratio as follows: firstly, we store the maximum profit of a request if it is positive together with the origin zone of this request. This is the profit that would be obtained if the request was served by the closest vehicle. Secondly, we store the theoretical profits that would be obtained from subsequent requests originating in the same zone if a vehicle was available at the same position as the vehicle closest to the original request. We store the theoretical profits for the ten time steps after the original request appears. Thirdly, we obtain the overprofits by subtracting the profit of the original request from the theoretical profits. We only count positive overprofits subsequently, as we only consider requests that would be more profitable than the original request. We sum these overprofits conditional on whether the original request is accepted or rejected. Finally, we divide the overprofit after a rejection by the overprofit after an acceptance.

A numerical illustration is as follows: consider a request, which could be served by a vehicle in the same zone with an initial profit of 10 USD, but the operator rejects this request. From the same zone, three further requests appear within the ten subsequent time steps. Using a vehicle within the same zone, they could be served with a profit of 5 USD, 12 USD, and 14 USD, respectively. These numbers are the theoretical profits. The associated overprofits are 0 USD, 2 USD, and 4 USD. Therefore, the total overprofit compared to the original request is 6 USD. Now, consider a second request, which is accepted by the operator, with an initial profit of 10 USD and subsequent theoretical profits of 8 USD, 11 USD, and 12 USD. The overperformance for this request is 3 USD. If these are the only two profitable requests available, the overperformance ratio is 6 divided by 3, which equals 2. As the overperformance ratio is larger than one, the subsequent requests after the rejection are more profitable than those after the acceptance. Accordingly, whenever the overperformance ratio is larger than one, we can conclude that the analyzed algorithm is better at taking anticipative decisions than a greedy algorithm.

### Acknowledgments

We thank the CORAIL research group at Polytechnique Montréal for valuable comments and discussions. The work of Heiko Hoppe was supported by a scholarship from the Max Weber-Programm Bayern.

### References

- Javier Alonso-Mora, Alex Wallar, and Daniela Rus. Predictive routing for autonomous mobility-on-demand systems with ride-sharing. In *2017 IEEE/RSJ International Conference on Intelligent Robots and Systems (IROS)*, 2017.
- Yu-Han Chang, Tracey Ho, and Leslie Kaelbling. All learning is Local: Multi-agent Learning in Global Reward Games. In *Advances in Neural Information Processing Systems (NeurIPS)*, volume 16, 2003.
- Petros Christodoulou. Soft Actor-Critic for Discrete Action Settings. arXiv preprint at arXiv, 2019. URL [arXiv:1910.07207v2](https://arxiv.org/abs/1910.07207v2).
- Tobias Enders, James Harrison, Marco Pavone, and Maximilian Schiffer. Hybrid Multi-agent Deep Reinforcement Learning for Autonomous Mobility on Demand Systems. In *Proceedings of The*



- 5th Annual Learning for Dynamics and Control Conference (L4DC)*, volume 211 of *Proceedings of Machine Learning Research (PMLR)*, 2023.
- Jakob Foerster, Gregory Farquhar, Triantafyllos Afouras, Nantas Nardelli, and Shimon Whiteson. Counterfactual Multi-Agent Policy Gradients. *Proceedings of the AAAI Conference on Artificial Intelligence*, 32(1), 2018.
- Tuomas Haarnoja, Aurick Zhou, Pieter Abbeel, and Sergey Levine. Soft Actor-Critic: Off-Policy Maximum Entropy Deep Reinforcement Learning with a Stochastic Actor. In *Proceedings of the 35th International Conference on Machine Learning (ICML)*, 2018.
- Dylan Hadfield-Menell, Smitha Milli, Pieter Abbeel, Stuart J. Russell, and Anca Dragan. Inverse Reward Design. In *Advances in Neural Information Processing Systems (NeurIPS)*, volume 30, 2017.
- Sihong He, Yue Wang, Shuo Han, Shaofeng Zou, and Fei Miao. A Robust and Constrained Multi-Agent Reinforcement Learning Electric Vehicle Rebalancing Method in AMoD Systems. arXiv preprint at arXiv, 2022. URL [arXiv:2209.08230](https://arxiv.org/abs/2209.08230).
- Yan Jiao, Xiaocheng Tang, Zhiwei (Tony) Qin, Shuaiji Li, Fan Zhang, Hongtu Zhu, and Jieping Ye. Real-world ride-hailing vehicle repositioning using deep reinforcement learning. *Transportation Research Part C: Emerging Technologies*, 130, 2021.
- Kai Jungel, Axel Parmentier, Maximilian Schiffer, and Thibaut Vidal. Learning-based Online Optimization for Autonomous Mobility-on-Demand Fleet Control. arXiv preprint at arXiv, 2023. URL [arXiv:2302.03963](https://arxiv.org/abs/2302.03963).
- Jelle R. Kok and Nikos Vlassis. Collaborative Multiagent Reinforcement Learning by Payoff Propagation. *Journal of Machine Learning Research (JMLR)*, 7, 2006.
- Der-Horng Lee, Hao Wang, Ruey Long Cheu, and Siew Hoon Teo. Taxi Dispatch System Based on Current Demands and Real-Time Traffic Conditions. *Transportation Research Record: Journal of the Transportation Research Board*, 1882(1), 2004.
- Enming Liang, Kexin Wen, William H. K. Lam, Agachai Sumalee, and Renxin Zhong. An Integrated Reinforcement Learning and Centralized Programming Approach for Online Taxi Dispatching. *IEEE Transactions on Neural Networks and Learning Systems*, 33(9), 2022.
- Ziqi Liao. Real-time taxi dispatching using Global Positioning Systems. *Communications of the ACM*, 46(5), 2003.
- Xiaomin Lin, Peter A. Beling, and Randy Cogill. Multiagent Inverse Reinforcement Learning for Two-Person Zero-Sum Games. *IEEE Transactions on Games*, 10(1), 2018.
- Karina Meneses-Cime, Bilin Aksun Guvenc, and Levent Guvenc. Optimization of On-Demand Shared Autonomous Vehicle Deployments Utilizing Reinforcement Learning. *Sensors*, 22(21), 2022.
- Andrew Y. Ng and Stuart J. Russell. Algorithms for Inverse Reinforcement Learning. In *Proceedings of the Seventeenth International Conference on Machine Learning (ICML)*, 2000.

- Duc Thien Nguyen, Akshat Kumar, and Hoong Chuin Lau. Credit Assignment For Collective Multiagent RL With Global Rewards. In *Advances in Neural Information Processing Systems (NeurIPS)*, volume 31, 2018.
- NYC TLC. Trip Record Data. Online, 2015. URL <https://www.nyc.gov/site/tlc/about/tlc-trip-record-data.page>.
- Tabish Rashid, Mikayel Samvelyan, Christian Schroeder De Witt, Gregory Farquhar, Jakob Foerster, and Shimon Whiteson. Monotonic Value Function Factorisation for Deep Multi-Agent Reinforcement Learning. *Journal of Machine Learning Research (JMLR)*, 21, 2020.
- Soheil Sadeghi Eshkevari, Xiaocheng Tang, Zhiwei Qin, Jinhan Mei, Cheng Zhang, Qianying Meng, and Jia Xu. Reinforcement Learning in the Wild: Scalable RL Dispatching Algorithm Deployed in Ridehailing Marketplace. In *Proceedings of the 28th ACM SIGKDD Conference on Knowledge Discovery and Data Mining*, 2022.
- Kyunghwan Son, Daewoo Kim, Wan Ju Kang, David Earl Hostallero, and Yung Yi. QTRAN: Learning to Factorize with Transformation for Cooperative Multi-Agent Reinforcement Learning. In *Proceedings of the 36th International Conference on Machine Learning (ICML)*, 2019.
- Jianyu Su, Stephen Adams, and Peter Beling. Value-Decomposition Multi-Agent Actor-Critics. *Proceedings of the AAAI Conference on Artificial Intelligence*, 35(13), 2021.
- Peter Sunehag, Guy Lever, Audrunas Gruslys, Wojciech Marian Czarnecki, Vinicius Zambaldi, Max Jaderberg, Marc Lanctot, Nicolas Sonnerat, Joel Z. Leibo, Karl Tuyls, and Thore Graepel. Value-Decomposition Networks For Cooperative Multi-Agent Learning Based On Team Reward. In *Proceedings of the 17th International Conference on Autonomous Agents and MultiAgent Systems*, 2018.
- Xiaocheng Tang, Zhiwei (Tony) Qin, Fan Zhang, Zhaodong Wang, Zhe Xu, Yintai Ma, Hongtu Zhu, and Jieping Ye. A Deep Value-network Based Approach for Multi-Driver Order Dispatching. In *Proceedings of the 25th ACM SIGKDD International Conference on Knowledge Discovery & Data Mining*, 2019.
- Matthew Tsao, Ramon Iglesias, and Marco Pavone. Stochastic Model Predictive Control for Autonomous Mobility on Demand. In *2018 21st International Conference on Intelligent Transportation Systems (ITSC)*, 2018.
- Zhaodong Wang, Zhiwei Qin, Xiaocheng Tang, Jieping Ye, and Hongtu Zhu. Deep Reinforcement Learning with Knowledge Transfer for Online Rides Order Dispatching. In *2018 IEEE International Conference on Data Mining (ICDM)*, 2018.
- Gerhard Weiß. Distributed Reinforcement Learning. *The Biology and Technology of Intelligent Autonomous Agents*, 1995.
- David H. Wolpert and Kagan Tumer. An Introduction to Collective Intelligence. Techreport NASA-ARC-IC-99-63, NASA, 1999.
- David H. Wolpert and Kagan Tumer. Optimal Payoff Functions For Members Of Collectives. *Advances in Complex Systems*, 04(02n03), 2001.

Cathy Wu, Aravind Rajeswaran, Yan Duan, Vikash Kumar, Alexandre M. Bayen, Sham Kakade, Igor Mordatch, and Pieter Abbeel. Variance Reduction for Policy Gradient with Action-Dependent Factorized Baselines. In *6th International Conference on Learning Representations (ICLR)*, 2018.

Zhe Xu, Zhixin Li, Qingwen Guan, Dingshui Zhang, Qiang Li, Junxiao Nan, Chunyang Liu, Wei Bian, and Jieping Ye. Large-Scale Order Dispatch in On-Demand Ride-Hailing Platforms. In *Proceedings of the 24th ACM SIGKDD International Conference on Knowledge Discovery & Data Mining*, 2018.

Lingyu Zhang, Tao Hu, Yue Min, Guobin Wu, Junying Zhang, Pengcheng Feng, Pinghua Gong, and Jieping Ye. A Taxi Order Dispatch Model based On Combinatorial Optimization. In *Proceedings of the 23rd ACM SIGKDD International Conference on Knowledge Discovery and Data Mining*, 2017.